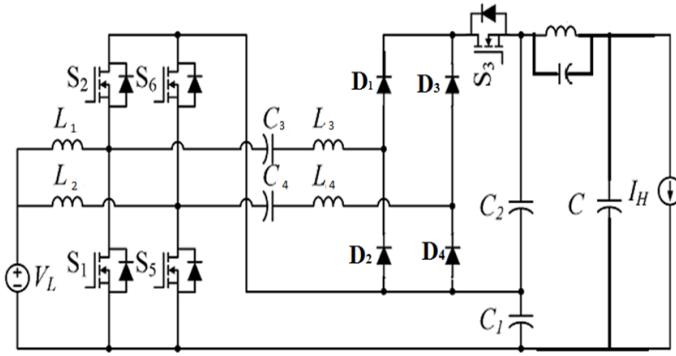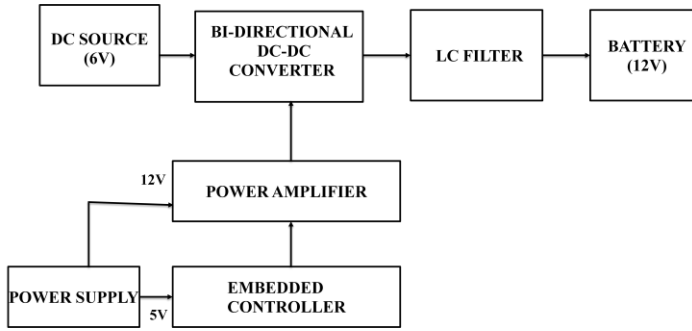Fig 1: Circuit diagram of proposed converter

Fig 2: Block diagram of proposed converter

a. Operating Principle

The capacitances C_1, C_2 and C are large enough so that voltages V_{C1}, V_{C2}, and V_C across them are constant during the switching period T_S. In boost mode, Low-Voltage Side (LVS) switches S_1, S_2, S_5 and S_6 are operated with asymmetrical complementary switching with duty cycles of D (duty cycle) and 1−D respectively. Initially when S_1 is turned on, inductor currents i_{Lf} starts to increase and i_{La} starts to decrease respectively. The slopes are determined by the following equations:

$$\frac{di_{L1}}{dt} = \frac{V_L}{L_1} \qquad [1]$$

$$\frac{di_{L2}}{dt} = \frac{V_L}{L_2} \qquad [2]$$

$$\frac{di_{L3}}{dt} = \frac{V_{C3}-V_{C1}-V_{C2}}{L_3} \qquad [3]$$

$$\frac{di_{L4}}{dt} = \frac{V_{C4}-V_{C1}-V_{C2}}{L_4} \qquad [4]$$

To analyze the steady state operation of the converter, the following assumptions are made [10]:
1) The output capacitor C is large enough to assume that the output voltage V_o is constant and ripple free.
2) The main inductor Lf is large enough to be treated as a constant-current source I_{Lf}.
3) Main inductor L_f is much greater than resonant inductor L_r.
4) The semiconductor devices and the reactive elements are ideal.

b. Voltage Conversion Ratio
The HVS voltage is given by the following equation:

$$V_H = \frac{2}{1-D_{eff}} . V_L \qquad [5]$$

where the effective duty is defined as follows:

$$D_{eff} = D - d_3 \qquad [6]$$

where d_3 means duty loss at switch S_3. The output voltage can also be expressed as follows:

$$V_H = \frac{2}{1-D} . V_L - \Delta V \qquad [7]$$

where ΔV is the voltage drop caused by the duty loss.
The voltage drop ΔV can be obtained as follows:

$$\Delta V = \frac{2V_L * d_3}{(1-D)(1-D+d_3)} \qquad [8]$$

Because the average current of C_3, C_4 and C_2 is zero, the average absolute currents of HVS switches can be expressed as follows:

$$\frac{1}{T_S}\int_0^{T_S}|i_{S3}| \, dt = I_H \qquad [9]$$

where $I_H = V_H / R_H$.

A. Mode I operation

The diode across switches S_1 and S_5 conducts initially as shown in fig. 3(a). The current flows through both L1, C_3, L_3, D_1 and L2, C_4, L_4, D_3 to switch S_3 to C_1, C_2 and then to the load.
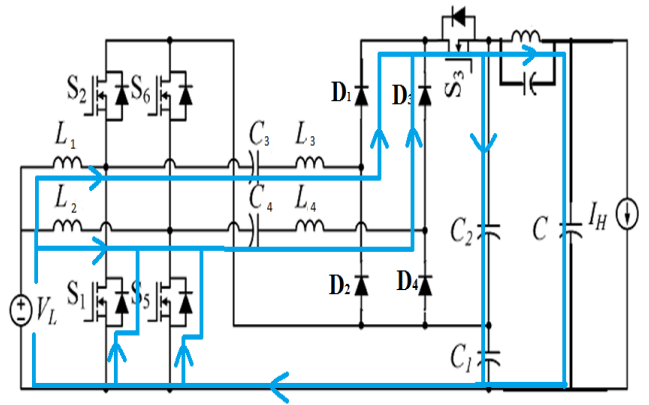

Fig 3(a): Mode I operation

B. Mode II operation

The switches S_1 and S_5 start conducting. The input voltage is fed to the input inductors L_1 and L_2 to store charge as well as to the load.
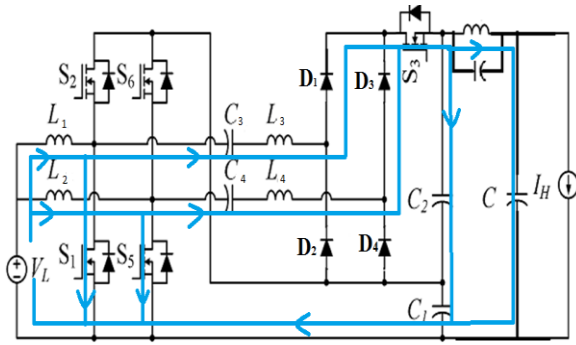
Fig 3(b): Mode II operation
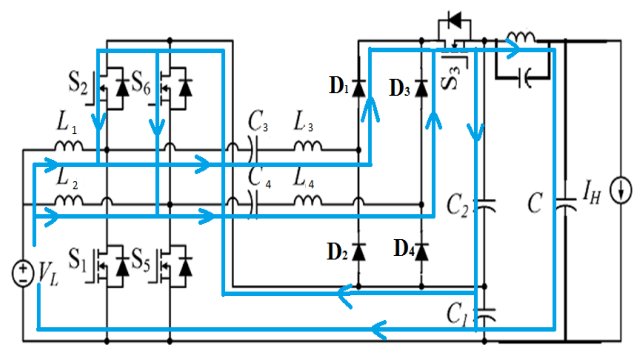
C. Mode III operation

The capacitor C_1 starts discharging where the current flows load and input switches. The current through switches S_1 and S_5 is the sum of input current and current through capacitor C_1 respectively.
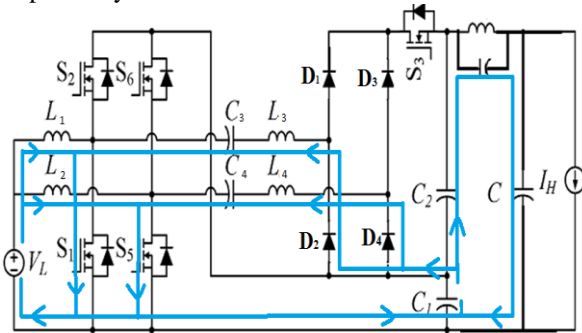
Fig 3(c): Mode III operation

D. Mode IV operation

The diodes across switches S_2 and S_6 allows current to flow from input to capacitor C_1. The HVS diodes D_2 and D_4 conduct.
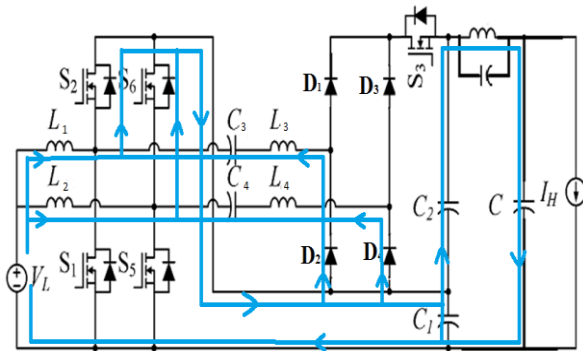
Fig 3(d): Mode IV operation

E. Mode V operation

The switches S_2 and S_6 are turned on which forward biases the diodes D_1 and D_3 respectively. Switch S_3 is turned on so that the current flows to the battery load.

Fig 3(e): Mode V operation

3. SIMULATION RESULTS

The interleaving technique can be applied to reduce the size of passive components and current stresses. A 5.9W prototype of the BDC shown in Fig.1 has been simulated according to the following specification:

$P_o = 5.92$ W, $f_s = 1$ kHz, $V_H = 14.21$ V, $V_L = 6$ V, $L_f = 50$ µH, $L_a = 50$ µH, $C_a = 10$ µF, $C_1 = C_2 = 10$ µF.
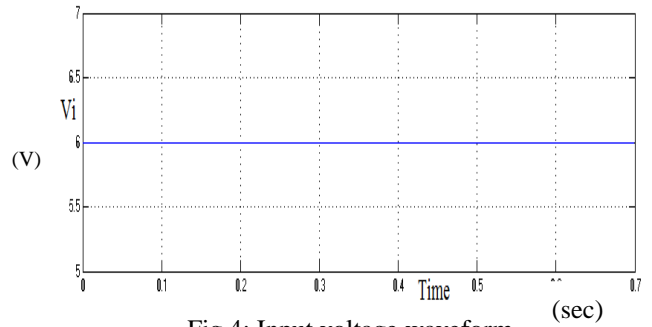
Fig 4: Input voltage waveform
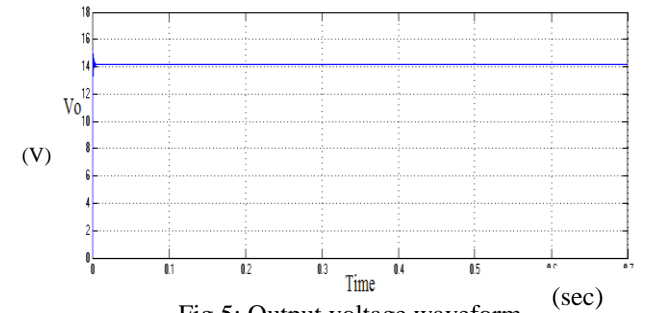
Fig 5: Output voltage waveform
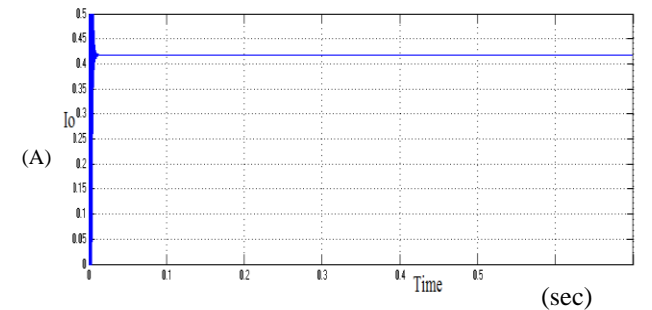
Fig 6: Output current waveform
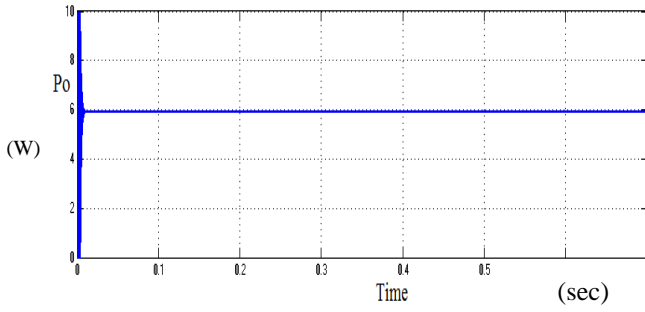
Fig 7: Output power waveform

The pulses given to the gate of each switch is shown in fig.10. The gate pulses to switches S_1 is complement to switch S_2. The gate pulse given upper switches S_2 and S_6 and the gate pulse given lower switches S_1 and S_5 are identical.
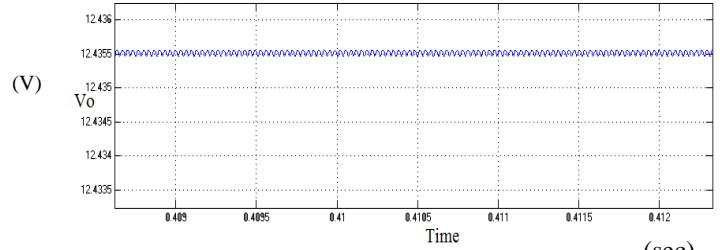
Fig 8: Ripple in output voltage waveform
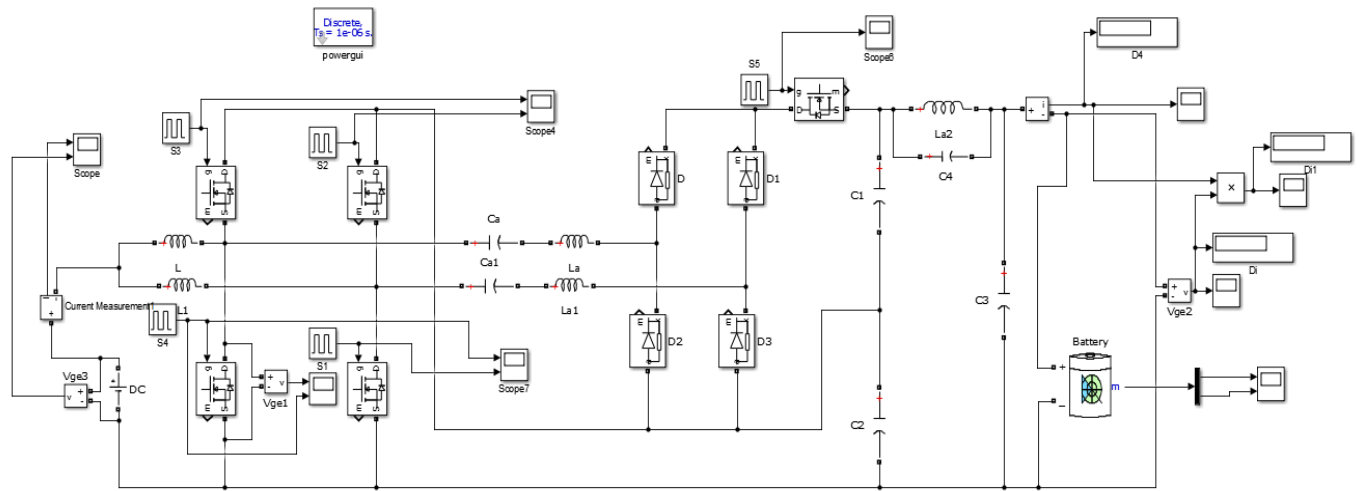
Fig 9: Simulink diagram of proposed circuit
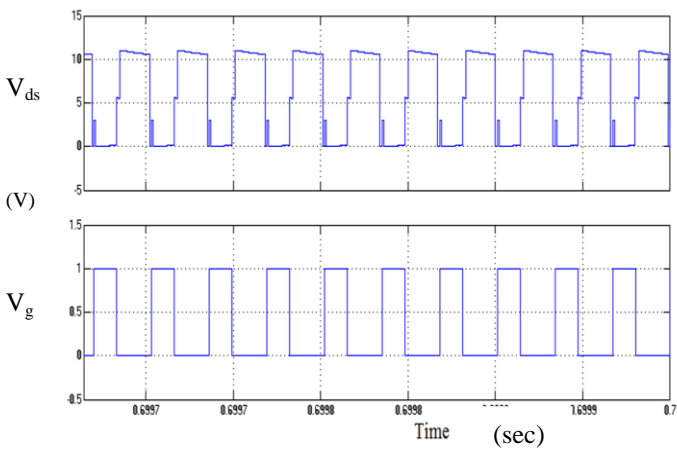
Fig 9: Drain to source voltage and switching pulse of single switch

6V DC input is given to get an output voltage of 14V, power obtained of 6W approximately with a 0.42A output current. The drain to source voltage applied to each MOSFET switch is 10V.
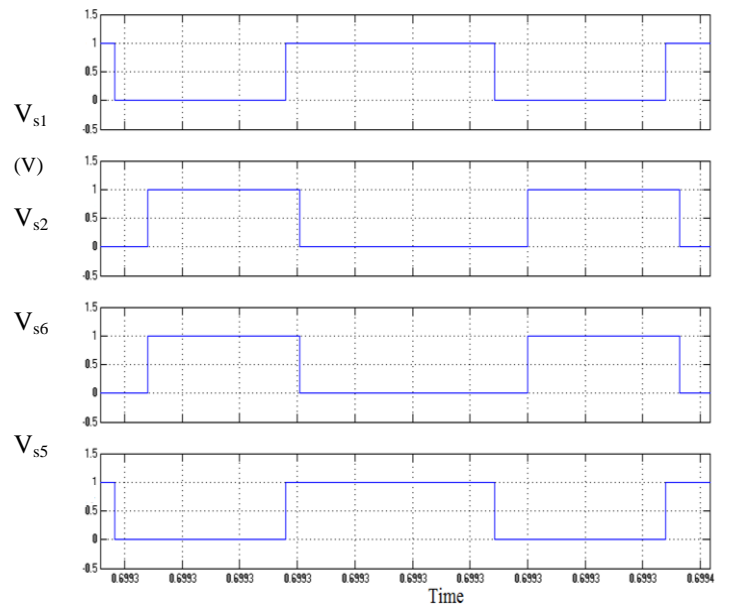
Fig 10: Switching pulses to four switches

4. HARDWARE RESULTS

The simulated prototype has been implemented and the output is verified. The output of the setup is given to a rechargeable battery used in motorcycle.
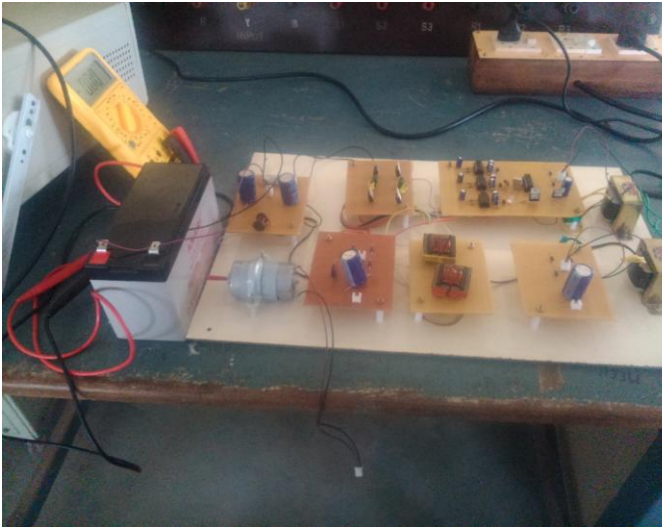
Fig 11: Complete hardware setup
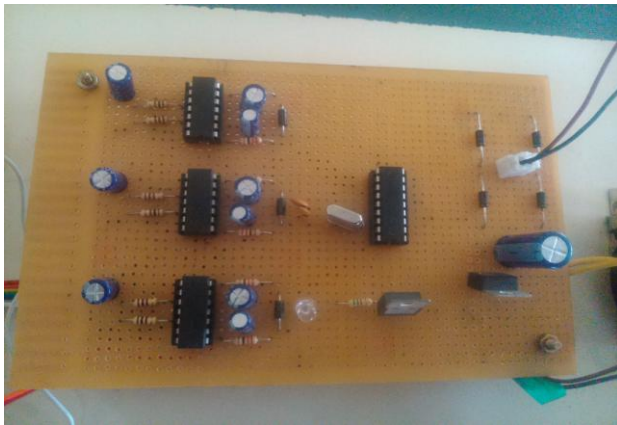
Fig 12: PIC microcontroller circuit
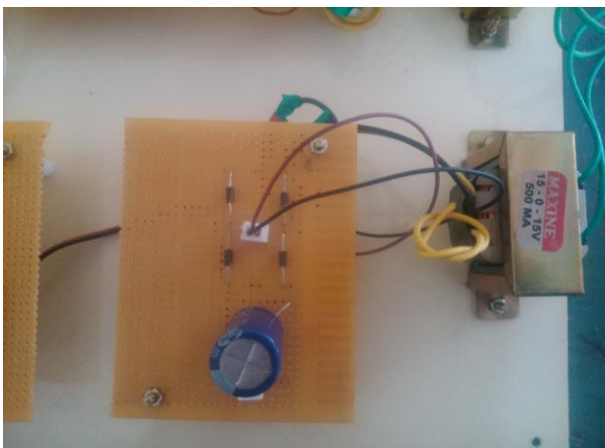
Fig 13: Input power circuit
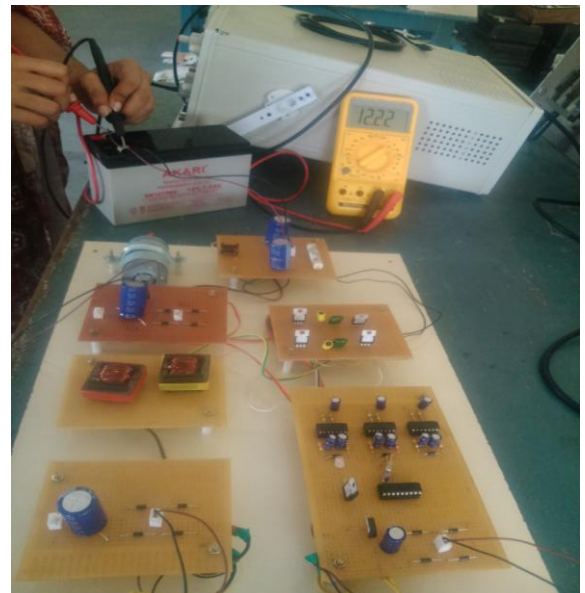
Fig 15: Output 12V in multimeter

Fig 16: Output 12V in CRO

5. CONCLUSION

In this paper, a non-isolated soft switching BDC has been proposed for high-voltage gain and low-power applications. The proposed converter can achieve ZVS turn on of all switches and ZCS turn off some switches in both boost and buck operations. An optimized switching sequence has been presented along with an intermediate switching pattern to carry out seamless mode change. ZVS reduces the switching current and frequency and a high output voltage is obtained. A 5.9W prototype of the proposed converter has been simulated to justify the proposed operation. A 6V DC input voltage is boosted to 14V and fed to the resistor after filtering. The converter used for low power applications can be modified by isolating the LVS and HVS using a transformer for high power applications.

REFERENCES

[1] "High Gain Soft-Switching Bidirectional DC–DC Converter for Eco-Friendly Vehicles",Minho Kwon, Secheol Oh, and Sewan Choi, in power electronics, vol. 29, no. 4, April 2014

[2] J. Zhang, R. Y. Kim, and J. S. Lai, "High-Power density design of a soft-switching high-power bidirectional DC-DC converter," in *Proc IEEE Power Electron. Spec. Conf.*, 2006, vol. 2, pp. 1–7.

[3] Y. Du, X. Zhou, S. Bai, S. Lukic, and A. Huang, "Review of non-isolated bi-directionalDC–DC converters for plug-in hybrid electric vehicle charge station application at municipal parking decks," in *Proc. 25th IEEE Appl.Power Electron. Conf. Expo.*, 2010, pp. 1145–1151.

[4] Prius Battery Specifications. (2013). [Online]. Available: http://www.toyotapriusbattery.com

[5] P. Das, B. Laan, S. A. Mousavi, and G. Moschopoulos, "A nonisolated bidirectional ZVS-PWM active clampedDC–DC converter," *IEEE Trans. Power Electron.*, vol. 24, no. 2, pp. 553–558, Feb. 2009.

[6] B. L. Narasimharaju, S. P. Dubey, and S. P. Singh, "Design and analysis of coupled inductor bidirectionalDC-DC convertor for high-voltage diversity applications," *IET. Power Electron.*, vol. 5, no. 7, pp. 998–1007, Aug. 2012.

[7] F. L. Luo, H. Ye, and M. H. Rashid, "Switched capacitor four-quadrant DC/DC Luo-converter", in *Proc IEEE IAS. Ind. Appl. Conf.*, 1999, vol. 3, pp. 1653–1660.

[8] I. Kim, J. Kim, E. Nho, and H. Kim, "Analysis and design of softswitched PWM sepic DC-DC converter," *J. Power Electron.*, vol. 10, no. 5, pp. 461–467, Sep. 2010.

[9] Luciano Schuch,Cassiano Rech, Helio Leaes Hey, Hilton Abilio Grundling, Humberto Pinheiro and Jose Renes Pinheiro, "Analysis and Design of a New High Efficiency Bidirectional Integrated ZVT PWM Converter for DC-Bus and Battery Bank Interface," IEEE Transactions on industry applications, vol.42,September/October 2006.

[10] Zhiling Liao and Xinbo Ruan, " A Novel Power Management Control Strategy for Stand-Alone Photovoltaic Power System," IEEE 2009.